

## Internal Motion of DNA in Bacteriophages\*

(Received for publication, November 7, 1983)

Ikuo Ashikawa, Taiji Furuno, Kazuhiko Kinoshita, Jr., Akira Ikegami‡, Hideo Takahashi§, and Hideo Akutsu¶

From the Institute of Physical and Chemical Research, Hirosawa 2-1, Wako-shi, Saitama 351, Japan, the §Institute of Applied Microbiology, University of Tokyo, Bunkyo-ku, Tokyo 113, Japan, and the ¶Institute for Protein Research, Osaka University, Suita-shi, Osaka 565, Japan

We have investigated internal motion of DNA in bacteriophages by measuring fluorescence anisotropy decays of intercalated ethidium. The results showed large suppression of the internal motion of the inner DNA; the interhelix interaction of the DNA in the phage head is considered to enhance the effective viscosity of the DNA rod and to restrict the angle of the internal motion. Considering that the observed internal motion arises mainly from torsional motion of the DNA, we have calculated the movable angles of the torsional motion (the standard deviation of the torsional motion) of the DNA in the phage heads. The magnitude of the calculated movable angles indicates the extent of suppression of the DNA movement in the phage head; in  $\lambda$  wild type phage, the DNA is packed most rigidly in the head and the motion is found to be restricted most severely. In a deletion mutant of  $\lambda$  phage, whose inner DNA content is deficient by 17.6%, steric hindrance from the interhelix DNA interaction is decreased, and the DNA can move more easily. In T4 wild type phage, although the extent of condensation of the inner DNA is the same as that in  $\lambda$  wild type phage, the DNA was fairly mobile. The presence of glucosylated hydroxymethylcytosine is suggested to influence the rigidity of the inner DNA or packaging mode of the DNA in the T4 head.

DNA of double-stranded DNA bacteriophages are typically several hundred times longer than the phage head, and DNA strands have been thought to adopt some tertiary structure in the head (Earnshaw and Casjens, 1980). Several studies have appeared which aimed at determining the packing geometry of nucleic acids in phage particles by x-ray diffraction and electron microscopy (North and Rich, 1961; Richards *et al.*, 1973; Earnshaw *et al.*, 1976; Earnshaw and Harrison, 1977; Earnshaw *et al.*, 1978). According to these studies, the DNA in phage heads is ordered in a closely packed structure. The DNA array in several phages, such as  $\lambda$  or T even phages, consists of parallel strands which extend over 10 nm and are rigidly held in close contact with the protein shell.

Interhelix distances of DNA in bacteriophages have been determined precisely by x-ray diffraction studies. Earnshaw and Harrison (1977) determined the interhelix distances of several deletion mutants of  $\lambda$  phage, whose DNA content is deficient by 12 or 22% compared with that of  $\lambda$  wild type phage, and found that, in  $\lambda$  mutants containing less than a

full genome, the local packing distance increases correspondingly. Their result clearly demonstrated that the extent of the condensation of the DNA rods in these bacteriophages was determined by the amount of the inner DNA, the rods of which repel each other.

Internal motion of DNA in solution has been investigated recently by using techniques such as NMR (Early and Kearns, 1979; Hogan and Jardetzky, 1979, 1980b; Bolton and James, 1980; Opella *et al.*, 1981), fluorescence depolarization (Wahl *et al.*, 1970; Thomas *et al.*, 1980; Millar *et al.*, 1980, 1982), ESR (Robinson *et al.*, 1980), and triplet anisotropy decays (Hogan *et al.*, 1982). Among these techniques, nanosecond fluorescence depolarization studies of intercalated ethidium have revealed the DNA motion in the nanosecond range, the main component of which is considered to be torsional motion of the DNA rod. This technique is a powerful method for the investigation of the internal motion of DNA in a rather complicated biological system, such as DNA in cell nuclei and in viruses.

In this article, we demonstrate an application of nanosecond fluorescence depolarization of intercalated ethidium in order to elucidate dynamics of DNA in several kinds of bacteriophages ( $\lambda$ ,  $\lambda$  deletion mutant ( $\lambda\Delta$  phage), T4D, and T4 mutant phage (T4dC mutant) which has normal cytosine in its DNA instead of glucosylated hydroxymethylcytosine). Although packaging of the DNA in these phage heads has been clarified considerably, little information is available on dynamic state of the packaged DNA. There is only one study which treats dynamics of the DNA in bacteriophages; Akutsu *et al.* (1980)<sup>1</sup> investigated dynamics of phosphate moiety of the DNA in bacteriophages T4, PM2, and  $\lambda$  using <sup>31</sup>P NMR. According to their study, phosphate motion of DNAs in these phage heads was severely restricted compared with DNA in solution, but not so restricted as that of solid DNA. Measuring anisotropy decay of the intercalated ethidium, we found that the internal motion of the DNA in phage heads was largely restricted as compared with the isolated DNA. We have found that the extent of restriction of the internal motion of the DNA in bacteriophages differed from each other and that the extent of the restriction reflected the interhelix distance of the DNA rods or glucosylation of the bases in the DNA.

### MATERIALS AND METHODS

**Preparation of Samples**—Bacteriophages  $\lambda$  and  $\lambda$  deletion mutant ( $\lambda\Delta 52401cI, S7$ ) were prepared according to the procedure reported (Goldberg and Howe, 1969), and only a summary of the procedures is described below. We prepared  $\lambda$  wild type phage using *Escherichia coli* (C600 $\lambda$ cI<sub>857</sub>S7) (kindly donated by Dr. Katsura, University of Tokyo) as a host cell, which contains  $\lambda$  DNA in its chromosomal DNA.  $\lambda$  wild type phage ( $\lambda$ cI<sub>857</sub>S7) was produced by shifting the

\* The costs of publication of this article were defrayed in part by the payment of page charges. This article must therefore be hereby marked "advertisement" in accordance with 18 U.S.C. Section 1734 solely to indicate this fact.

‡ To whom correspondence should be addressed.

<sup>1</sup> H. Akutsu, N. Katsutani, Y. Kyogoku, and A. Matsushiro, unpublished result.

culture temperature to 42 °C.  $\lambda$  deletion mutant ( $\lambda\Delta$ cI<sub>S7</sub>), the whose chromosomal DNA length is reduced by 17.6% (Yamagishi *et al.*, 1977), was obtained as a recombinant of  $\lambda\Delta$ 52401cI (kindly donated by Dr. Yamagishi, Kyoto University) and  $\lambda$ cI<sub>S7</sub>. We prepared this phage by infecting the phage to *E. coli* C600. After lysing the host cell with chloroform, we washed the lysate by centrifugation and purified the phages by centrifugation at 35,000 rpm on a stepwise gradient of CsCl for 1 h. That the obtained  $\lambda\Delta$  phage was actually the deletion mutant of  $\lambda$  wild type phage was checked by performing a thermal stability test of this phage. Bacteriophage T4D wild type and T4dC mutant (T4dC(+)=amC87(42<sup>-</sup>),amE51(56<sup>-</sup>), denB-s19,unf39(alc); Takahashi and Saito, 1982), which has cytosine bases in its DNA instead of glucosylated hydroxymethylcytosine bases, were obtained following the procedure of Coppo *et al.* (1973). We infected bacteriophage T4D and T4dC mutant to *E. coli* B and a restriction deficient mutant of *E. coli* (B834=sup<sup>0</sup>r<sup>-</sup>), respectively. After lysing the host cell, we washed the lysate by centrifugation with buffer solutions (M9 salts (Coppo *et al.*, 1973)) several times.

Bacteriophage DNA was prepared as follows. The phages were disrupted by treatment with 1 mM EDTA, 0.1% sodium dodecyl sulfate at 65 °C, and the outpoured DNA was isolated with chloroform/isoamyl alcohol (24:1).

Chicken erythrocyte long DNA was isolated by the method of Kay *et al.* (1952). Chicken erythrocyte chromatin DNA (short DNA) was isolated from oligonucleosomes. Sedimentation coefficients of the long DNA and the short DNA were 20.0 and 8.2 S, respectively, in 5 mM Tris, 100 mM NaCl, 1 mM EDTA, pH 7.5, at 20 °C. Molecular weights were considered to be about  $6 \times 10^6$  for the long DNA and  $5 \times 10^5$  for the short DNA.

**Preparation of a DNA Aggregate (or Bundle) and of a DNA-Spermidine Complex**—A DNA aggregate was formed by adding ethanol to chicken erythrocyte chromatin DNA (short DNA) in 5 mM Tris, 0.2 mM EDTA. Final concentration of ethanol was 75% by volume. When we used long DNA to form the aggregate, it made an insoluble aggregate and the sample could not be used for measurements.

A DNA-spermidine complex was made by adding spermidine solution to chicken erythrocyte chromatin DNA (short DNA) in 5 mM Tris, 0.2 mM EDTA. Final concentration of the added spermidine was 0.8 mM. In this case also, only short DNA made a soluble complex. In these preparations, ethidium dye was added to DNA before condensation.

**Measurements of Fluorescence**—Fluorescence anisotropy measurements of the added dye in bacteriophages or isolated DNA from the phages were performed in buffer solutions of 10 mM Tris, 10 mM NaCl, 5 or 20 mM MgSO<sub>4</sub>, pH 7.4. DNA concentrations of the samples were 0.1~0.3 mg/ml, and the DNA to added ethidium bromide ratio ([phosphate of DNA]/[dye]) was about 2000~750. In these low concentrations of added dye, energy transfer between the intercalated dyes was negligible. In anisotropy measurements of the phages, we added DNase I ( $\approx 2 \mu\text{g/ml}$ ) to the samples. Added DNase I completely digested the free DNA from the ruptured phages and inhibited intercalation of ethidium in free DNA. We did not add gelatin, which has been thought to stabilize phage samples (Hall and Schellman, 1982), to the sample solution because added gelatin would change the viscosity of the sample solution. Cuvette temperature was kept at 20 °C.

In the case of fluorescence anisotropy measurements of the dye in the DNA aggregate collapsed by ethanol or the DNA-spermidine complex, sample DNA concentrations were 0.05~0.2 mg/ml, and [phosphate of DNA]/[dye] values were 2000~500. Buffer conditions were 75% ethanol, 1 mM Tris, 0.04 mM EDTA, pH 7.5, for the DNA aggregate by ethanol and 0.8 mM spermidine, 5 mM Tris, 0.2 mM EDTA, pH 7.5, for the DNA-spermidine complex. In these samples also, the cuvette was kept at 20 °C.

Fluorescence anisotropy decay was measured with a single photon-counting apparatus (Kinosita *et al.*, 1981). The nanosecond light pulses were provided by free running discharge in H<sub>2</sub> gas. In the present work, we used as an excitation source 520 nm components of pulsed light, and emission above 560 nm was collected. The principal components of polarized fluorescence decay,  $I_1(t)$  and  $I_2(t)$ , were simultaneously measured with two photomultiplier tubes. The total fluorescence decay curve,  $I_T(t)$ , and the anisotropy decay curve,  $R(t)$ , were calculated as follows.

$$I_T(t) = I_1(t) + 2I_2(t) \quad (1)$$

$$I_D(t) = I_1(t) - I_2(t) \quad (2)$$

$$R(t) = I_D(t)/I_T(t) \quad (3)$$

The detailed descriptions of deconvolution and least squares procedures for data analysis have been described earlier (Ashikawa *et al.*, 1983b).

In the case of DNAs in the phage heads or in the DNA aggregate, since the affinity of the dye to the DNA was reduced, only 20~60% of the added dyes could be intercalated in the DNA. We therefore subtracted the fluorescence components of the free dye from the observed fluorescence decay curves prior to the analysis as follows. Because the fluorescence lifetime of the free dye ( $\approx 1.7$  ns) was much shorter than the lifetime of the bound dye (23~24 ns), the ratio of the free dye in the sample was determined by the lifetime analysis of the  $I_T(t)$  curve. Considering that anisotropy from the free dye was almost zero and it should not contribute to the  $I_D(t)$  curve, we subtracted the fluorescence component of the free dye from the  $I_T(t)$  curve. Although the precise correction was rather difficult and anisotropy values near 0 ns look too high (see figures), the correction was significant only at 0~10 ns, and the corrected decay curves after 10 ns were completely identical to the uncorrected ones. Obtained rigidities from the least squares calculation did not change whether we took the anisotropy near 0 ns into account or not; the ambiguities of the data near 0 ns did not influence the results.

**Analysis of the Observed Anisotropy Decay Curve**—Details of the deconvolution and least squares fitting procedures were described earlier (Ashikawa *et al.*, 1983b). In order to characterize the internal motion of DNA, we adopted the following analysis.

The major part of the anisotropy decay of the intercalated ethidium has been considered to arise from the torsional motion of the DNA (Barkley and Zimm, 1979; Allison and Schurr, 1979). For DNA in solution, if the transition moment of the intercalated ethidium is nearly perpendicular to the helix axis of the DNA (in the case of B-form DNA, this assumption seems valid (Dickerson *et al.*, 1982)), the observed anisotropy decay arising from the torsional motion of the DNA is known to follow the equation (Barkley and Zimm, 1979; Allison and Schurr, 1979):

$$r(t) = r_0(0.75 \exp(-(t/\phi_1)^{1/2}) + 0.25) \quad (4)$$

where  $\phi_1 = \pi^2 b^2 \eta C / 4k_B^2 T^2$  ( $T$  is the absolute temperature,  $k_B$  the Boltzmann constant,  $b$  the radius of the DNA,  $\eta$  the viscosity of the solution, and  $C$  the torsional rigidity of the DNA). Fitting Equation 4 to the observed anisotropy decay, we obtained  $\phi_1$ . From this value, we calculated the torsional rigidity  $C$ . In this calculation, the hydrodynamic radius of the DNA ( $b$ ) was assumed to be 1.35 nm (Millar *et al.*, 1980; Ashikawa *et al.*, 1983b).

In the case of the DNA in bacteriophages or in the DNA aggregate (or DNA bundle) collapsed by ethanol, free rotation around the helix axis of the DNA is probably inhibited by interhelix DNA interactions, and we think that Equation 4 cannot be used for the analysis. In fact, we could not successfully fit Equation 4 to the decay curves of these kinds of the condensed DNAs, especially DNA in  $\lambda$  wild type phage and in T4dC mutant phage. The anisotropy values of these DNAs did not seem to decay to as low as 0.09 (see Fig. 1 and Fig. 7), which is the  $r_\infty$  value for freely movable torsional motion ( $r_0$  is assumed to be 0.36). Therefore, we think that the internal motion of the condensed DNAs, such as DNA in phages or in the DNA aggregate, undergoes torsional motion with a restricted movable angle. Since an exact expression for the anisotropy decay for such a restricted torsional motion has not been solved yet, we assumed the following description:

$$r(t) = r_0 (a_1 \exp(-(t/\phi_1)^{1/2}) + a_2) \quad (5)$$

where  $a_1$ ,  $a_2$  ( $=1 - a_1$ ), and  $\phi_1$  are the parameters that characterize the internal motion. In this expression, the term  $\exp(-t^{1/2})$  was inferred from Equation 4. The constant  $a_2$  in this expression was considered to arise from the restricted motion; when the angle of a motion is restricted, its anisotropy value at infinite time ( $r_\infty$ ) is raised from zero to a constant (Kinosita *et al.*, 1977). Equation 5 has been applied to the analysis of the anisotropy decay of the torsional motion of the dye in the DNA fixed ends, where the movable angle was also restricted due to the presence of fixed ends (Ashikawa *et al.*, 1983b). The observed increase in the constant ( $r_\infty/r_0$ ) from 0.25 in Equation 4 to  $a_2$  was considered to result from the restriction of the movable angle. We fitted Equation 5 to the condensed form of DNA (DNA in bacteriophages, etc.) and calculated  $\phi_1$  and  $a_2$  (i.e.  $r_\infty/r_0$ ).

From the value of  $a_2$  ( $=r_\infty/r_0$ ), we calculated the movable angle of

the DNA via:

$$r_{\infty}/r_0 = 0.75 \exp(-\Gamma(\infty)) + 0.25 \quad (6)$$

where  $\Gamma(\infty)$  is the torsional decay function at infinite time (Barkley and Zimm, 1979; Ashikawa *et al.*, 1983b). The standard deviation (movable angle) of the torsional angle at infinite time is calculated to be  $\Gamma(\infty)/2^{1/2}$ .

In the least squares fit of Equation 5 to the observed decay curves, we fixed  $r_0$  to 0.36. Although the experimental  $r_0$  (*i.e.*  $R(0)$ ) values of DNA in phages could not be observed in our experiment,  $r_0$  values of intercalated ethidium in B-form DNA free in solution and complexed with proteins were always 0.36 (Ashikawa *et al.*, 1983b).

**Measurements of X-ray Diffraction**—In measurements of x-ray diffraction patterns of the DNAs in the phages and in the DNA aggregates, the samples were contained in thin wall quartz capillary tubes ( $\approx 1$ -mm diameter). The concentrations of the samples were 50–100 mg/ml. X-ray beams were provided from a rotating anode x-ray generator (Rigaku-Denki, RU-200H), and the x-ray diffraction patterns were recorded with a position-sensitive proportional counter. Details of this system has been described elsewhere (Furuno *et al.*, 1983).

## RESULTS AND DISCUSSION

**Anisotropy Decay of DNA in  $\lambda$  and  $\lambda\Delta$  Phages**—Intercalating dyes have been known to bind to DNA in bacteriophages. Shurdov and Popova (1982) investigated the binding sites of these intercalating probes by cross-linking 8-methoxypsoralen in the  $\lambda$  phage head. They concluded that binding sites were fairly widespread in the phage DNA, the amount of the bound dye in the surface of the DNA core being only twice as much as that in the inner most layer. In bacteriophages, ethidium dye has been reported to bind only to DNA (Hall and Schellman, 1982). These results suggest that the anisotropy decay of intercalated ethidium reflects the internal motion of almost whole DNA in bacteriophages.

Fig. 1 shows the anisotropy decay curves of the dye in  $\lambda$

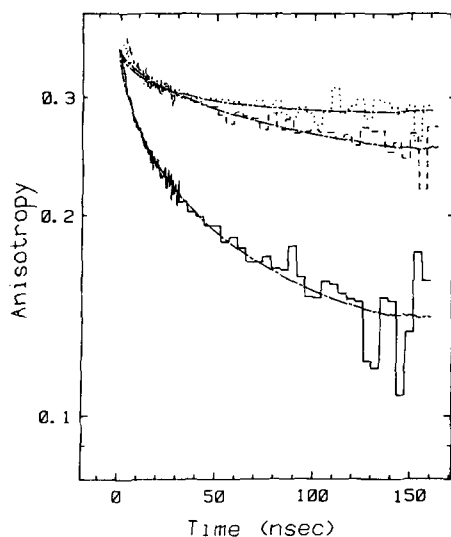


FIG. 1. Fluorescence anisotropy decay curves of intercalated ethidium in  $\lambda$  wild type phage (dotted line),  $\lambda$  deletion mutant ( $\lambda\Delta$ cIS7) (dashed line), and isolated  $\lambda$  DNA (solid line). Sample concentrations were 0.1–0.3 mg/ml, and measurements were performed in 10 mM Tris, 10 mM NaCl, 20 mM  $\text{MgSO}_4$ , pH 7.5, at 20 °C. [Phosphate of DNA]/[dye] was 2000–1750. The anisotropy values after 30 ns are averaged over 10 channels (1 ns equals 2.32 channels). The lines (---) represent the results of least square fit with Equation 5 or 4 to the decays of the DNA in phage heads or of the isolate  $\lambda$  DNA, respectively.

TABLE I

Obtained values of the parameters  $a_1$ ,  $a_2$ , and  $\phi_1$  in Equation 4 or 5 of DNA in bacteriophages in the ethanol-collapsed aggregate and in the spermidine-collapsed complex and of the isolated DNAs from them

Sample	$a_1$	$a_2$	$\phi_1$	Movable angle
			ns	
$\lambda$ wild	0.238	0.762	24.3	15°
$\lambda\Delta$	0.699	0.302	413.0	108°
$\lambda$ DNA	0.750	0.250	46.2	
T4 wild type	0.452	0.548	15.7	37°
T4 wild type DNA	0.750	0.250	63.5	
T4dC mutant	0.229	0.771	18.0	15°
T4dC mutant DNA	0.750	0.250	49.5	
Ethanol-collapsed aggregate	0.526	0.474	737.5	49°
Spermidine-collapsed complex	0.464	0.536	11.0	39°
Long DNA (chicken erythrocyte)	0.750	0.250	54.7	

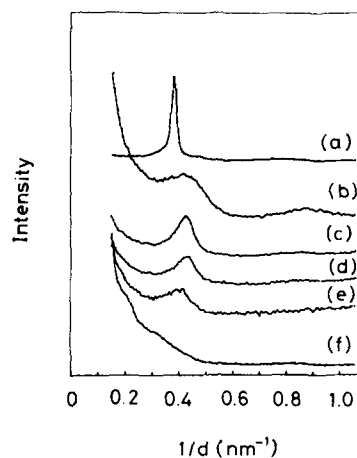


FIG. 2. X-ray diffraction patterns of DNAs recorded with a position-sensitive proportional counter. The concentration of the samples were 50–10 mg/ml. All experiments were performed at 23 °C. a, the DNA-spermidine complex; b, the ethanol-collapsed aggregate; c, T4 wild type phage; d, T4dC mutant; e,  $\lambda$  wild type phage; f,  $\lambda$  deletion mutant ( $\lambda\Delta$ cIS7).

wild type phage, in  $\lambda\Delta$  phage, and in purified DNA from  $\lambda$  phage, together with the respective fitting curves. Calculated parameters are listed in Table I. From the obtained  $\phi_1$  value, the torsional rigidity of the isolated  $\lambda$  DNA was calculated to be  $1.6 \times 10^{-19}$  erg·cm. This is almost the same value as that for calf thymus DNA in 0.1 M NaCl ( $1.4 \times 10^{-19}$  erg·cm). The torsional rigidities reported by other laboratories are also almost the same (*i.e.*  $1.29 \times 10^{-19}$  erg·cm for  $\phi 29$  DNA (Thomas *et al.*, 1980) and  $1.43 \times 10^{-19}$  erg·cm for calf thymus DNA (Millar *et al.*, 1982)). As to  $\lambda$  wild type phage, we can recognize that the motion of the inner DNA was largely suppressed compared with free DNA. The observed anisotropy of  $\lambda$  wild type phage reached an almost constant value beyond 50 ns. The estimated  $r_{\infty}/r_0$  value of  $\lambda$  wild type phage was fairly high, which indicated that the movable angle of the motion was restricted severely. Fig. 2 shows an x-ray diffraction pattern from DNA in the phage head. Diffraction spacing of the DNA in  $\lambda$  wild type phage was 2.4 nm (Fig. 2e), and since the inner DNA is considered to be arranged in a hexagonal packing (North and Rich, 1961), the interhelix distance of the DNA was calculated to be 2.8 nm, which is the same value as reported by Earnshaw and Harrison (1977). The radius of nonhydrated B-form DNA is known to be 2.0 nm (Dickerson *et al.*, 1982). Considering the hydration around the DNA, there is probably contact of DNA rods with surrounding rods. The observed suppression of the movement of

the inner DNA may result from this contact of a DNA rod with adjacent DNA rods. The condensation of the inner DNA seems to enhance the effective viscosity of the DNA rod and to restrict the movable angle of the torsional motion.

To confirm this idea, we measured the anisotropy decay of intercalated ethidium in  $\lambda\Delta$  phage. The length of the DNA in this phage is reduced by 17.6% compared with that in  $\lambda$  wild type phage. Although the diffraction pattern from  $\lambda\Delta$  phage was poor because of the small amount of the samples, it shows an increased interhelix distance (Fig. 2). The diffraction spacings of inner DNAs reported by Earnshaw and Harrison (1977) were 2.6 and 2.5 nm for  $\lambda$  deletion mutants whose inner DNAs were reduced by 22 and 12%, respectively, compared with  $\lambda$  wild type phage. Considering these values, the interhelix distance of the DNA rods in  $\lambda\Delta$  phage, whose DNA length is intermediate between the two deletion mutants of Earnshaw and Harrison (1977), should be reduced by about 0.15 nm. In the case of  $\lambda\Delta$  phage, while the anisotropy decay was not so extensive as that of free DNA, it exhibited more enhanced decay than that of the DNA in  $\lambda$  wild type phage (Fig. 1). In particular, the anisotropy decayed slowly even after 100 ns. As seen in Table I, the  $r_{\infty}/r_0$  value for  $\lambda\Delta$  phage was calculated to be much smaller than that for  $\lambda$  wild type phage and to be close to that for the isolated  $\lambda$  DNA. The increased mobility of the DNA rod probably resulted from decreased interhelix DNA interaction.

Using NMR, Akutsu *et al.*<sup>1</sup> have investigated the mobility of the  $^{31}\text{P}$  moiety of the DNA in  $\lambda$  phage head. Chemical shift anisotropy of  $^{31}\text{P}$  of the DNA in the phage head was averaged only slightly, in contrast to isolated DNA. However, the observed  $T_1$  value of  $^{31}\text{P}$  of the DNA in the phage was close to that of isolated DNA. These facts indicate that although the movement of the DNA rod is highly suppressed, the flexibility of the phosphate backbone of the DNA is not as restricted as in free DNA. Recently, Rill *et al.* (1983) examined effects of intermolecular DNA interactions on the motional dynamics of double-stranded DNA with defined lengths by measuring  $^{13}\text{C}$  and  $^{31}\text{P}$  NMR. They concluded that restriction of the motion of various atoms in DNA changed as the bundling of the sample DNA proceeded and that phosphate motion in DNA was relatively insensitive to the intermolecular interactions.

Akutsu *et al.*<sup>1</sup> found that as temperature increases, the chemical shift anisotropy and  $T_1$  of  $^{31}\text{P}$  of the DNA within  $\lambda$  phage change in such a way as to suggest enhanced mobility of the DNA. Our result from anisotropy measurements basically supports their conclusion that the DNA motion was highly suppressed in the bacteriophage head. However, we could not observe the temperature dependence of the anisotropy decay of the intercalated dye in the DNA in  $\lambda$  phage from 8 to 37 °C (data not shown). These differences may be explained as follows. As pointed out by Hogan and Jardetzky (1980a), DNA motion revealed by  $^{31}\text{P}$  NMR is mainly local motion, *i.e.* motion of the phosphate backbone of DNA. Therefore, movement of the DNA rod in the phage head, which was observed by our anisotropy study, may not change with temperature, and local movement will be enhanced by the increase in temperature. DiVerdi and Opella (1981) reported temperature dependence of  $^{31}\text{P}$  and  $^2\text{H}$  chemical shift anisotropy of solid state DNA; when the temperature of B-form DNA in the solid state was raised from 20 to 50 °C, the  $^{31}\text{P}$  NMR chemical shift powder pattern became significantly averaged by motions that were rapid compared with  $10^4$  Hz, and the  $^2\text{H}$  powder pattern from  $^2\text{H}$  at purine C-8 was not averaged. There exist two interpretations for their result: 1) the motion of the DNA backbone moiety is more sensitive to

the temperature increase than the movement of the whole DNA rod, and 2) the DNA motion faster than  $10^6$  Hz is not sensitive to the temperature increase (the  $^2\text{H}$  NMR chemical shift powder pattern is considered to be averaged only by a motion which is rapid compared with  $10^6$  Hz). The origin of the temperature independence of the anisotropy decay of the dye in the DNA in  $\lambda$  wild type phage may be the same as that of the case reported by DiVerdi and Opella (1981).

**Anisotropy Decay of the Dye in the DNA Aggregate and the DNA-Spermidine Complex**—In order to settle the relationship between the DNA motion and the interhelix distance of the DNA rod more clearly, we measured anisotropy decay of the intercalated dye in condensed DNA of simpler systems.

DNA has been reported to form a crystalline precipitate in aqueous alcohol solution (Lerman *et al.*, 1976). We made a DNA aggregate by adding ethanol up to 75% in the presence of several millimolar  $\text{Na}^+$ . When we used short DNA (several hundred base pairs), a soluble aggregate was obtained. The sedimentation velocity of this aggregate was 70.5 S in 75% ethanol, and CD measurement of this sample revealed that the DNA was in B-form (Fig. 3). In Fig. 2b, an x-ray diffraction pattern of this aggregate is shown, and from this figure we recognize that DNA in the aggregate was aligned parallel. The interhelix distance of the DNA was calculated to be 2.7 nm (hexagonal packing being assumed (Lerman *et al.*, 1976)). This interhelix distance is almost the same as that of the DNA rods in  $\lambda$  wild type phage. The anisotropy decay curve of the dye in the aggregate is shown in Fig. 4, together with the decay curve of free long chicken erythrocyte DNA in 5 mM Tris, 0.2 mM EDTA, pH 7.5. Fitting Equation 4 or 5 to these decay curves, we obtained the parameters listed in Table I. The anisotropy decay was as highly suppressed as in the  $\lambda$  phage. Although the detailed decay profile of the dye in the DNA aggregate is different (see  $a_2$  value in Table I), this decay curve clearly indicates that the suppression of the movement of the DNA rod in bacteriophages originates from steric hindrance by surrounding DNA chains.

In the case of the DNA-spermidine complex, the DNA rods were shown to be arrayed parallel with each other (Fig. 2a). However, the interhelix distance of the DNA in this complex was larger than the DNA aggregate or DNA in  $\lambda$  phage by 0.3 nm. The DNA in this complex has been known to be the B-

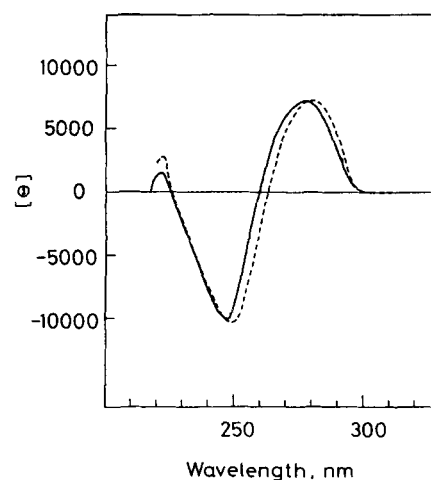


FIG. 3. Circular dichroism spectra of the DNA aggregate collapsed by ethanol (dashed line) and of the chicken erythrocyte short DNA in solution (solid line). Sample concentrations were 0.07 mg/ml. Measurements were performed in 75% ethanol, 1 mM Tris, 0.04 mM EDTA, pH 7.5 for the aggregate and 5 mM Tris, 0.2 mM EDTA, pH 7.5 for DNA in solution at room temperature.

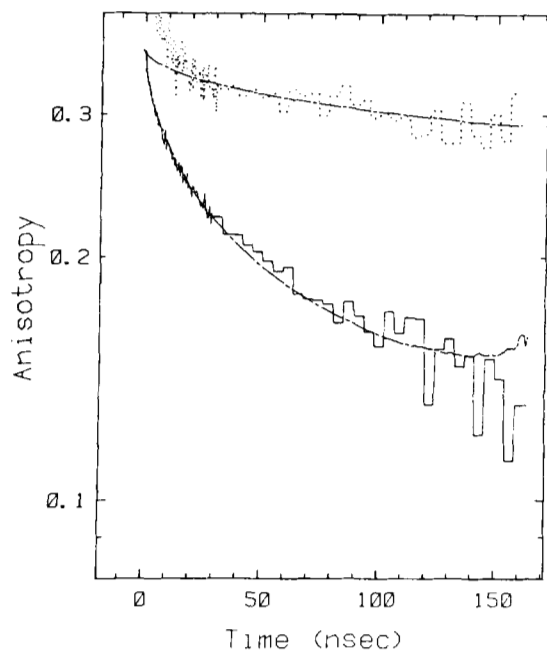


FIG. 4. Fluorescence anisotropy decay curves of intercalated ethidium in the aggregate collapsed by ethanol (dotted line) and in chicken erythrocyte long DNA in solution (solid line). Sample concentrations were 0.05–0.2 mg/ml, and measurements were performed in 75% ethanol, 1 mM Tris, 0.04 mM EDTA, pH 7.5, for the aggregate and 5 mM Tris, 0.2 mM EDTA, pH 7.5, for DNA in solution at 20 °C. [Phosphate of DNA]/[dye] was 2000–1500. The dashed lines represent the results of least squares fit with Equation 5 or 4 to the observed decays of the DNA aggregate or the DNA in solution, respectively.

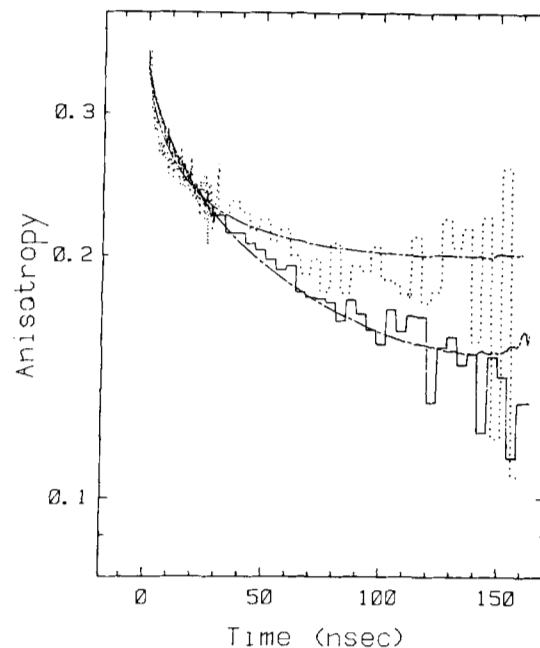


FIG. 5. Fluorescence anisotropy decay curves of intercalated ethidium in the DNA-spermidine complex (dotted line) and in chicken erythrocyte long DNA in solution (solid line). The anisotropy decay curve of the complex is the corrected one as described in the text. Sample concentrations were 0.05–0.2 mg/ml, and measurements were performed in 0.8 mM spermidine, 5 mM Tris, 0.2 mM EDTA, pH 7.5, for the complex and in 5 mM Tris, 0.2 mM EDTA for the free DNA at 20 °C. [Phosphate of DNA]/[dye] was 2000–1500. The dashed lines represent the results of least squares fit with Equation 5 or 4 to the observed decay of the DNA-spermidine complex or the DNA in solution, respectively.

form (Gosule and Schellman, 1978). The anisotropy decay curve of the dye in this complex is shown in Fig. 5, together with that in free DNA in solution. In this complex, a portion of the added dye was intercalated to small sized complexes or free DNA which was not removable by ultracentrifugation of the sample. Therefore, we corrected the anisotropy decay curve, following the procedure described below, so that anisotropy decay from the dye intercalated only in the large complex would be obtained; the fraction of the dye intercalated in the small sized complexes or free DNA was estimated to be 40% by comparing the ethidium fluorescence intensity and lifetime from the supernatant and from the pellet of the sample after ultracentrifugation (20,000 rpm for 1 h). We obtained the true anisotropy decay curve of the dye in the large complex by subtracting the anisotropy decay of the dye in the small sized complexes from the observed decay curve taking the fraction of the dye in the small sized complexes into account. Although this correction for ethidium in the small sized complexes seems rather complex, the effect of the correction on the decay curve was small; we think that the corrected decay curve represents the DNA motion in the DNA-spermidine complex fairly well. The corrected anisotropy decayed more rapidly and largely than that of  $\lambda$  phage or that of the ethanol-collapsed aggregate. This result clearly indicates that lowered steric hindrance from the surrounding DNA enhanced the internal motion of the DNA in the condensed state.

In the DNA-spermidine complex, DNA is considered to be collapsed by ionic interaction between spermidine and the phosphate groups of the DNA. Since there was little suppression of the anisotropy decay of the dye, it may be concluded that internal motion of DNA was not so hindered by ionic bondings. This observation resembles the case of histone-

DNA interaction in a nucleosome core particle; the torsional motion of the DNA around a histone octamer was not suppressed completely by ionic bondings between DNA and histone proteins (Wang *et al.*, 1982; Ashikawa *et al.*, 1983a, 1983b).

*Anisotropy Decay of Ethidium in T4 Wild Type Phage and T4dC Mutant*—As mentioned in the previous section, it is suggested that the extent of suppression of the internal motion of DNA in its condensed (or collapsed) state is related to the interhelix distance of the DNA. In this section, we discuss whether this rule holds for another type of bacteriophage. We investigated the internal motion of the DNA in T4 phage. This phage adopts “headful packaging” of its DNA (Earnshaw and Casjens, 1980), and its DNA has glucosylated hydroxymethylcytosine residues instead of normal cytosines. Hall and Schellman (1982) suggest that the orientation of the packaged DNA bundle in T4 wild type phage is different from that in  $\lambda$  phage. The origin of this difference in packaging of DNA has not been clarified. The anisotropy decay curve of ethidium in T4 phage and that in the isolated DNA are shown in Fig. 6. The anisotropy of the dye in this phage decayed much faster and extensively than that of the dye in  $\lambda$  phage, while that of the isolated DNA decayed slightly slower than that of the isolated DNA form  $\lambda$  phage ( $\phi_1$  in Equation 4 was 46.2 ns for  $\lambda$  DNA and 63.5 ns for T4 wild type DNA). We now show that the observed enhanced mobility of the inner DNA did not arise from experimental artifacts; in order to check whether energy transfer between the dyes or light scattering from the sample influenced the decay curve, we made measurements in several different concentrations of ethidium or samples. Nearly the same steric hindrance exists in the DNA rod in T4 phage as in  $\lambda$  phage, since the interhelix distance

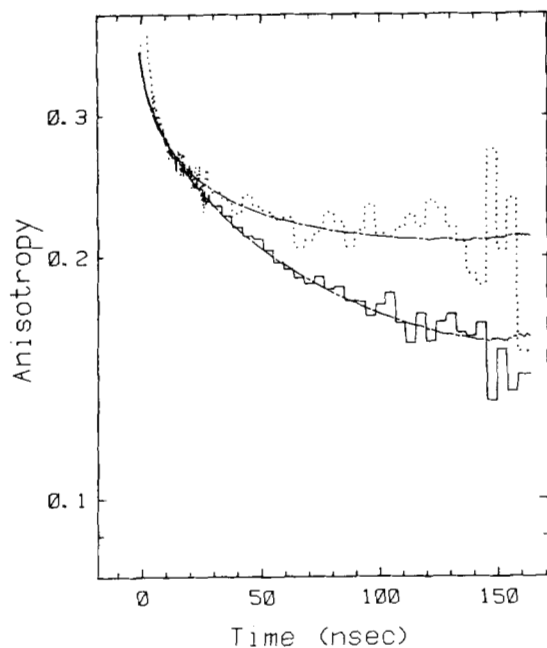


FIG. 6. Fluorescence anisotropy decay curves of the intercalated ethidium in T4 wild type phage (dotted line) and the isolated DNA from T4 phage (solid line). Sample concentrations were 0.1–0.3 mg/ml, and measurements were performed in 10 mM Tris, 10 mM NaCl, 5 mM MgSO<sub>4</sub>, pH 7.5, at 20 °C. [Phosphate of DNA]/[dye] was 2000–1750. The dashed lines represent the results of least squares fit with Equation 5 or 4 to the decay of the DNA in T4 phage or the decay of the isolated T4 DNA, respectively.

of the DNA in T4 phage was similar to or slightly smaller than that of the DNA in  $\lambda$  wild type phage (Fig. 2c). Therefore, in T4 phage the mobility of the inner DNA which was detected by anisotropy measurements does not obey the rule mentioned above.

In order to decide whether headful packaging or glucosylation of the DNA caused the enhanced mobility of the dye in T4 phage, we measured the anisotropy decay of ethidium in one kind of T4 mutant, T4dC, which has normal cytosine residues instead of glucosylated hydroxymethylcytosine residues in its DNA. Other properties of this mutant are considered to be the same as that of T4 wild phage (*i.e.* this phage adopts headful packaging). In fact, the interhelix distance and the extent of the inner DNA regularity were shown to be identical to that of T4 wild type phage (Fig. 2d). The decay curve obtained from this phage is shown in Fig. 7, together with the decay curve of the isolated DNA. The anisotropy decay of the dye in T4dC mutant was suppressed as severely as in  $\lambda$  wild type phage. Therefore, we concluded that the enhanced mobility of the dye in T4 wild type phage was caused solely by glucosylation of cytosine residues of its DNA.

There are at least two possible explanations for this enhanced mobility of the glucosylated DNA in T4 phage. One is that the presence of the glucose molecules changes the DNA structure in T4 wild type phage to a more flexible form. The other is that glucosylation of the bases influences the packaging of the inner DNA so that the dye could be intercalated in only flexible portions of the DNA in T4 wild type phage. If we assume that the distribution of the intercalated dye in T4dC mutant was identical to that in the wild type phage, the former explanation is favored. However, there is evidence which favors the latter explanation; Akutsu *et al.* (1980)<sup>1</sup> investigated the internal motion of the DNA in T4 and  $\lambda$  phage by using <sup>31</sup>P NMR. Although the motion detected by <sup>31</sup>P NMR may not be directly related to the movement of the

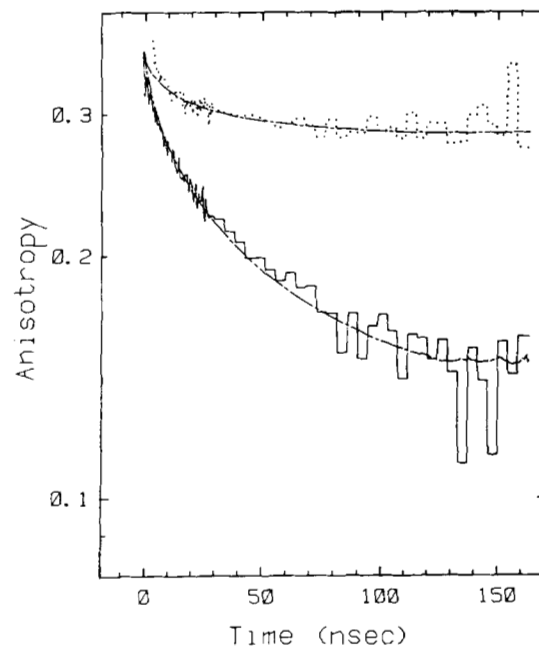


FIG. 7. Fluorescence anisotropy decay curves of intercalated ethidium in T4dC mutant (dotted line) and isolated DNA from this phage (solid line). Sample concentrations were 0.1–0.3 mg/ml, and measurements were performed in 10 mM Tris, 10 mM NaCl, 5 mM MgSO<sub>4</sub>, pH 7.5, at 20 °C. [Phosphate of DNA]/[dye] was 2000–1750. The dashed lines represent the results of least squares fit with Equation 5 or 4 to the decays of the DNA in T4dC mutant and the isolated DNA from this phage, respectively.

whole DNA rod, it may give some information about our interpretation of the DNA motion in T4 wild type phage. Their conclusion was that the mobility of the DNA within T4 phage was more restricted than that of  $\lambda$  phage. The NMR study gives information about the motion of the phosphate moiety of the whole DNA in bacteriophages. The result from the NMR study implies that the dye in the T4 wild type phage was not intercalated in the whole DNA but mainly in the flexible portion in the T4 phage. Hall and Schellman (1982) reported that the penetration speed of intercalated dyes in T4 phage was faster than that in  $\lambda$  phage; this result may suggest complexity of dye binding site in T4 phage.

Further study is required to clarify the reason for the enhanced mobility of the intercalated dye in T4 wild type phage.

*Characterization of the Internal Motion of the DNA in Bacteriophages*—The suppression of the motion of the DNA in bacteriophages and in the DNA aggregate is greater than that in free DNA. This suppression of movement is considered to arise from the contact of a DNA rod with surrounding rods, which enhances the effective viscosity around and restricts the movable angle of the DNA rod. In this section, we discuss the movable angle and the effective viscosity of the condensed DNA. The movable angle was calculated from the obtained  $a_2$  (*i.e.*  $r_\infty/r_0$ ) value, as mentioned under “Materials and Methods.” Results were 15° for  $\lambda$  wild type phage, 108° for  $\lambda\Delta$  phage, 37° for T4 wild type phage, 15° for T4dC mutant, 49° for the DNA aggregate (or bundle), and 39° for the DNA-spermidine complex. From these values, we can easily recognize that the motion of the DNAs in  $\lambda$  wild type phage and in T4dC mutant was suppressed the most. The movable angle of the torsional motion of the DNA in the ethanol-collapsed aggregate was not so small, although the decay in the 0 ~ 150-ns range was similar to that of DNA in  $\lambda$  wild type phage. In the case of  $\lambda\Delta$  phage, although the decay looks relatively

suppressed in its 0 ~ 150-ns region (Fig. 1), the movable angle was calculated to be 108°. From these results, it is concluded that a larger interhelix distance reduces the steric hindrance which determines the movable angle of the DNA.

The  $\phi_1$  value in Equation 4 or 5 is related to the  $C \cdot \eta$  (the product of the torsional rigidity and the effective viscosity) value of the DNA. In the case of free DNA in solution,  $\phi_1$  in Equation 4 is proportional to  $C \cdot \eta$ . However, in a restricted motion, such as a motion of DNA in bacteriophages, a calculated correlation time is not directly related to  $C \cdot \eta$  (Kinosita *et al.*, 1977). Actually, the correlation times ( $\phi_1$  in Equation 5) of  $\lambda$  phage and T4dC mutant were smaller ones than that expected for the torsional motion of the DNA rods without restriction. If one wants to estimate the  $C \cdot \eta$  value of such DNAs, one must obtain the relationship between  $\phi_1$  and  $C \cdot \eta$ . As mentioned under "Materials and Methods," we have not yet solved the exact expression of the anisotropy decay of the torsional motion with restricted movable angles, and we could not estimate  $C \cdot \eta$  from the obtained  $\phi_1$  value. In this paper, we made a rough estimation of  $\eta$  values (*i.e.* value of effective viscosity) using the expression of the anisotropy decay of a dye in the midpoint of DNA fixed ends. The movable angle of the torsional motion in such a DNA is restricted by the fixed ends, and we think that the dye movement of this case rather resembles that of the motion with restricted movable angle. Although this assumption may be, strictly speaking, not valid, we think that we could roughly estimate  $C \cdot \eta$  values of the DNA in phages. The procedure of the calculation has been described earlier (Ashikawa *et al.*, 1983b). If we assume that torsional rigidities of the inner DNAs are not changed compared with that of free isolated DNAs, we can estimate effective viscosity ( $\eta$ ) around the DNA rod. The calculated effective viscosities around the DNA rods in phages, except T4 wild type, were 10–15 times as large as that of free DNA in solution (0.01 poise at 20 °C). This enhanced viscosity of the inner DNA could be caused by the interhelix DNA interactions (*i.e.* contact of a DNA rod with surrounding rods). In the case of T4 wild type phage, the calculated viscosity was only 1.5 times as large as that of DNA in solution. We cannot discriminate now whether or not this apparent low viscosity resulted from the reduced rigidity of the inner DNA.

*Acknowledgment*—We thank Professor Aizo Matsushiro of Osaka University for his aid in isolation of  $\lambda\Delta$  phage.

#### REFERENCES

- Akutsu, H., Satake, H., and Franklin, R. M. (1980) *Biochemistry* **19**, 5264–5270
- Allison, S. A., and Schurr, J. M. (1979) *Chem. Phys. Lipids* **41**, 35–59
- Ashikawa, I., Kinosita, K. Jr., Ikegami, A., Nishimura, Y., Tsuboi, M., Watanabe, K., and Iso, K. (1983a). *J. Biochem. (Tokyo)* **93**, 665–668
- Ashikawa, I., Kinosita, K. Jr., Ikegami, A., Nishimura, Y., Tsuboi, M., Watanabe, K., Iso, K., and Nakano, T. (1983b) *Biochemistry* **22**, 6018–6026
- Barkley, M. D., and Zimm, B. H. (1979) *J. Chem. Phys.* **70**, 2991–3007
- Bolton, P. H., and James, T. L. (1980) *J. Am. Chem. Soc.* **102**, 25–31
- Coppo, A., Manzi, A., Pulitzer, J. F., and Takahashi, H. (1973) *J. Mol. Biol.* **76**, 61–87
- Dickerson, R. E., Drew, H. R., Conner, B. N., Wing, R. M., Fratini, A. V., and Kopka, M. L. (1982) *Science (Wash. D. C.)* **216**, 475–485
- DiVerdi, J. A., and Opella, S. J. (1981) *J. Mol. Biol.* **149**, 307–311
- Early, T. A., and Kearns, D. R. (1979) *Proc. Natl. Acad. Sci. U. S. A.* **76**, 4170–4174
- Earnshaw, W. C., and Casjens, S. R. (1980) *Cell* **21**, 319–331
- Earnshaw, W. C., and Harrison, S. C. (1977) *Nature (Lond.)* **268**, 598–602
- Earnshaw, W. C., King, J., Harrison, S. C., and Eiserling, F. A. (1978) *Cell* **14**, 559–568
- Earnshaw, W. C., Casjens, S. R., and Harrison, S. C. (1976) *J. Mol. Biol.* **104**, 387–410
- Furuno, T., Ikegami, A., Kihara, H., Yoshida, M., and Kagawa, Y. (1983) *J. Mol. Biol.* **170**, 137–153
- Goldberg, A. R., and Howe, M. (1969) *Virology* **38**, 200–203
- Gosule, L. C., and Schellman, J. A. (1978) *J. Mol. Biol.* **121**, 311–326
- Hall, S. B., and Schellman, J. A. (1982) *Biopolymers* **21**, 2011–2031
- Hogan, M. E., and Jardetzky, O. (1979) *Proc. Natl. Acad. Sci. U. S. A.* **79**, 6341–6345
- Hogan, M. E., and Jardetzky, O. (1980a) *Biochemistry* **19**, 2079–2085
- Hogan, M. E., and Jardetzky, O. (1980b) *Biochemistry* **19**, 3460–3468
- Hogan, M., Wang, J., Austin, R. H., Monitto, C. L., and Hershkovitz, S. (1982) *Proc. Natl. Acad. Sci. U. S. A.* **79**, 3518–3522
- Kay, E. R. M., Simmons, N. S., and Dounce, A. L. (1952) *J. Am. Chem. Soc.* **74**, 1724–1726
- Kinosita, K., Jr., Kawato, S., and Ikegami, A. (1977) *Biophys. J.* **20**, 289–305
- Kinosita, K., Jr., Kataoka, R., Kimura, Y., Gotoh, O., and Ikegami, A. (1981) *Biochemistry* **20**, 4270–4277
- Lerman, L. S., Wilkerson, L. S., Venable, J. H., Jr., and Robinson, B. H. (1976) *J. Mol. Biol.* **108**, 271–293
- Millar, D. P., Robbins, R. J., and Zewail, A. H. (1980) *Proc. Natl. Acad. Sci. U. S. A.* **77**, 5593–5597
- Millar, D. P., Robbins, R. J., and Zewail, A. H. (1982) *J. Chem. Phys.* **76**, 2080–2094
- North, A. C. T., and Rich, A. (1961) *Nature (Lond.)* **191**, 1242–1245
- Opella, S. J., Wise, W. B., and DiVerdi, J. A. (1981) *Biochemistry* **20**, 284–290
- Richards, K. E., Williams, R. C., and Calendar, R. (1973) *J. Mol. Biol.* **78**, 255–259
- Rill, R. L., Hilliard, P. R., Jr., and Levy, G. C. (1983) *J. Biol. Chem.* **258**, 250–256
- Robinson, B. H., Lerman, L. S., Beth, A. H., Frisch, H. L., Dalton, L. R., and Auer, C. (1980) *J. Mol. Biol.* **139**, 19–44
- Shurdov, M. A., and Popova, T. G. (1982) *FEBS Lett.* **147**, 89–92
- Takahashi, H., and Saito, H. (1982) *Plasmid* **8**, 29–35
- Thomas, J. C., Allison, S. A., Appellof, C. J., and Schurr, J. M. (1980) *Biophys. Chem.* **12**, 177–188
- Wahl, P., Paoletti, J., and Lepeque, J.-B. (1970) *Proc. Natl. Acad. Sci. U. S. A.* **63**, 417–421
- Wang, J., Hogan, M., and Austin, R. H. (1982) *Proc. Natl. Acad. Sci. U. S. A.* **79**, 5896–5900
- Yamagishi, H., Ryo, K., and Inokuchi, H. (1977) in *Proceedings of the Second Taniguchi Symposium: Molecular Evolution and Polymorphism* (Kimura, N., ed) pp. 281–295, Mishima, Japan